

## LETTERS

The purpose of this Letters section is to provide rapid dissemination of important new results in the fields regularly covered by *Physics of Fluids A*. Results of extended research should not be presented as a series of letters in place of comprehensive articles. Letters cannot exceed three printed pages in length, including space allowed for title, figures, tables, references and an abstract limited to about 100 words. There is a three-month time limit, from date of receipt to acceptance, for processing Letter manuscripts. Authors must also submit a brief statement justifying rapid publication in the Letters section.

# Chaotic Lagrangian trajectories around an elliptical vortex patch embedded in a constant and uniform background shear flow

L. M. Polvani<sup>a)</sup> and J. Wisdom<sup>b)</sup>

Massachusetts Institute of Technology, Cambridge, Massachusetts 02139

(Received 5 May 1989; accepted 17 October 1989)

The Lagrangian flow around a Kida vortex [J. Phys. Soc. Jpn. **50**, 3517 (1981)], an elliptical two-dimensional vortex patch embedded in a uniform and constant background shear, is described by a nonintegrable two-degree-of-freedom Hamiltonian. For small values of shear, there exist large chaotic zones surrounding the vortex, often much larger than the vortex itself and extremely close to its boundary. Motion within the vortex is integrable. Implications for two-dimensional turbulence are discussed.

In recent years our understanding of incompressible two-dimensional turbulence at very high Reynolds numbers has been revolutionized by the advent of high-resolution numerical simulations<sup>1-5</sup> which have shown that an initially turbulent vorticity field evolves into one composed of a few isolated strong vortices moving in an extremely convoluted mass of weak vorticity filaments, whose dynamics has been demonstrated to be similar to those of a passive scalar.<sup>4</sup> Recent computations by Dritschel and Legras<sup>6</sup> indicate that coherent structures formed in two-dimensional turbulence tend to be rapidly stripped of the outer layers of vorticity, leaving very steep vorticity gradients. The Kida<sup>7</sup> vortex, a single inviscid elliptical patch of vorticity superimposed on a constant uniform background shear (rotation plus strain), is a simple model for an isolated vortex in the field of other distant vortices. In this Letter we present results on the Lagrangian flow in the velocity field of Kida vortices.

The problem of an elliptical patch of uniform vorticity superposed on a background with uniform vorticity and strain was investigated by Moore and Saffman,<sup>8</sup> who discovered stationary solutions, and later generalized by Kida,<sup>7</sup> who showed that, in the presence of a background streamfunction given by

$$\psi_B = \frac{1}{4}(\omega + s)x^2 + \frac{1}{4}(\omega - s)y^2, \quad (1)$$

where  $\omega$  and  $s$  are, respectively, the nondimensional<sup>9</sup> background vorticity and strain, an initially elliptical vortex retains its elliptical shape for all times. The aspect ratio  $\lambda$  ( $0 < \lambda < 1$ ) of the vortex and the angle  $\varphi$  between the major axis of the vortex and the  $x$  axis evolve in time according to

$$\frac{d\lambda}{dt} = -s\lambda \sin 2\varphi$$

and

$$(2)$$

$$\frac{d\varphi}{dt} = \Omega_K + \frac{1}{2}[\omega + s\lambda \cos 2\varphi],$$

where  $\Omega_K = \lambda / (1 + \lambda)^2$  is the angular velocity of an elliptical vortex patch in the absence of a shear (a Kirchhoff vortex), and  $\Lambda = (1 + \lambda^2) / (1 - \lambda^2)$ ; Kida<sup>7</sup> showed that (2) has a constant of the motion and can be recast in Hamiltonian form. Even for constant  $\omega$  and  $s$ , the phenomenology of its solutions is very rich. Briefly, at constant  $\omega$ , for values of the strain sufficiently large, all vortices are sheared away by the background flow (i.e.,  $\lambda \rightarrow 0$ ). On the other hand, for fixed  $s$ , given large enough background vorticity, the aspect ratio oscillates periodically while the vortex rotates. For comparable values of vorticity and shear the behavior is more complicated. The steady solutions of Moore and Saffman correspond to the critical points of (2). The linear and finite-amplitude stability of the Kida solutions have recently been investigated by Dritschel<sup>10</sup> and Meacham *et al.*<sup>11</sup> The examples presented in this Letter are all linearly stable.

We have studied the trajectories of fluid particles in the flow field of a Kida vortex for constant  $\omega$  and  $s$ . In Cartesian coordinates the equations of motion for a particle are

$$\frac{dx}{dt} = -\frac{\partial \Psi}{\partial y} \quad \text{and} \quad \frac{dy}{dt} = \frac{\partial \Psi}{\partial x}, \quad (3)$$

where the total streamfunction  $\Psi(x, y, t) = \psi_V(x, y, t) + \psi_B(x, y)$ , and the component  $\psi_V$  resulting from the vortex is the streamfunction of a Kirchhoff ellipse<sup>12</sup> of aspect ratio  $\lambda(t)$  and inclination  $\varphi(t)$ . For periodic  $(\lambda, \varphi)$  motion, the streamfunction  $\Psi$ , which plays the role of the Hamiltonian in (3), contains explicit periodic time dependence. Inside the vortex,  $\Psi$  is quadratic in  $x$  and  $y$ , and thus (3) is linear with periodic coefficients; therefore the motion inside the vortex is integrable. Outside the vortex (3) is nonlinear and explicitly time dependent; therefore one expects to find instances of deterministic chaotic advection.<sup>13,14</sup> Although several examples are now known of chaotic mixing in two-dimensional (2-D) inviscid flows due to time-dependent Eulerian streamfunctions composed of combinations of point

vortices,<sup>14,15</sup> we believe this to be the first example of chaotic advection resulting from a *finite-area* vortex whose velocity field is continuous in both space and time.

In order to numerically integrate (3), we have found it convenient to express the position of a fluid particle in terms of elliptical coordinates  $(\rho, \vartheta)$  rotating and stretching with the vortex itself. The transformation between the latter and the fixed Cartesian coordinates  $(x, y)$  is given by

$$\begin{aligned} x &= c \cosh \rho \cos \vartheta \cos \varphi - c \sinh \rho \sin \vartheta \sin \varphi, \\ y &= c \cosh \rho \cos \vartheta \cos \varphi - c \sinh \rho \sin \vartheta \sin \varphi, \end{aligned} \quad (4)$$

where  $c^2 = (1 - \lambda^2)/\lambda$ . Since the analytical form of  $\psi_V$  is given in terms of  $(\rho, \vartheta)$  and since the inversion of (4) is complicated, we have chosen to integrate the variables  $(\rho, \vartheta)$ —instead of  $(x, y)$ . Using (1), (3), and (4), one shows, after some algebra, that the evolution equations for  $\rho$  and  $\vartheta$  are given by

$$\begin{aligned} \frac{d\rho}{dt} &= \left( \frac{c^2 h^2}{2} \right) \left[ - \left( \Omega_K \sin 2\vartheta + 2c^{-2} \frac{\partial \psi_V}{\partial \vartheta} \right) \right. \\ &\quad \left. + \frac{1}{2} s \mathcal{F}(\rho, \vartheta, \varphi) \right], \\ \frac{d\vartheta}{dt} &= \left( \frac{c^2 h^2}{2} \right) \left[ - \left( \Omega_K \sinh 2\rho - 2c^{-2} \frac{\partial \psi_V}{\partial \rho} \right) \right. \\ &\quad \left. + \frac{1}{2} s \mathcal{G}(\rho, \vartheta, \varphi) \right], \end{aligned} \quad (5)$$

where

$$\begin{aligned} \mathcal{F} &= (\cosh 2\rho \sin 2\vartheta \cos 2\varphi + \sinh 2\rho \cos 2\vartheta \sin 2\varphi) \\ &\quad - \Lambda (\cos 2\varphi \sin 2\vartheta + \sinh 2\rho \sin 2\varphi), \\ \mathcal{G} &= (\sinh 2\rho \cos 2\vartheta \cos 2\varphi - \cosh 2\rho \sin 2\vartheta \sin 2\varphi) \\ &\quad + \Lambda (\sin 2\varphi \sin 2\vartheta - \sinh 2\rho \sin 2\varphi), \end{aligned}$$

and

$$c^2 h^2 = (\cosh^2 \rho - \cos^2 \vartheta)^{-1}.$$

Thus, instead of solving (3) directly, we have studied the equivalent two-degree-of-freedom Hamiltonian problem constituted by (2) and (5), which we have integrated numerically using the Bulirsch–Stoer algorithm<sup>16</sup> with relative accuracy of  $10^{-11}$  per time step.

Notice that when  $s = 0$  the ellipse rotates with angular velocity  $\Omega_K + (\frac{1}{2})\omega$  with a constant aspect ratio; this is a Kirchhoff vortex, for which the fluid motion is integrable. The corotating streamfunction of the Kirchhoff vortex possesses two hyperbolic critical points<sup>17</sup> located along the major axis on either side of the ellipse, as well as two elliptic critical points (designated “ghost vortices” by Melander *et al.*<sup>18</sup>); these are easily obtained as the stationary solutions of (5). In the presence of a small strain the Hamiltonian becomes time dependent. As is expected from the theory of perturbed Hamiltonian systems, the chaotic regions appear first around the separatrices connecting the hyperbolic points.

A remarkable result is that even small values of  $s$  can result in large chaotic zones. These chaotic zones may be exhibited by computing surfaces of section, obtained in this problem by strobing the particle trajectories at the period of

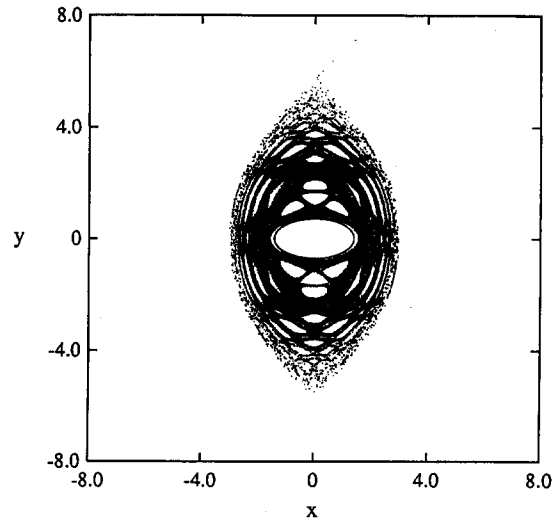


FIG. 1. The surface of section for an  $\omega = 0$ ,  $s = 0.03$  Kida vortex, with  $\lambda = 0.5$  at  $\varphi = 0$ . A single trajectory has been strobed with the period of rotation of the vortex, each dot representing the position of the fluid particle at each successive  $(\varphi, \lambda)$  period. The elliptical contour inside the chaotic zone indicates the boundary of the vortex.

the  $(\varphi, \lambda)$  motion, when  $\varphi = 0$ . An example is illustrated in Fig. 1, which shows a surface of section of a Kida vortex at  $\omega = 0$ ,  $s = 0.03$  and with  $\lambda = 0.5$  at  $\varphi = 0$ ; the aspect ratio varies in the interval  $0.435\ 251\ 48\dots < \lambda < 0.5$  and the period of revolution of the vortex differs only by half a percent from that of a Kirchhoff vortex with the same average aspect ratio. The time scale for the exponential divergence of nearby trajectories, as characterized by the largest Lyapunov exponent, is of the order of the  $(\varphi, \lambda)$  period. Thus the mixing in the chaotic zone is very rapid. For this particular case, the background field is hyperbolic and the particle eventually escapes from the vicinity of the vortex (see the top portion of Fig. 1).

Another particularly interesting finding is the unexpectedly large size of the chaotic zones for background strain and vorticity values in the vicinity of  $|\omega| = |s|$ ; this region corresponds to a background flow that is a simple shear (an unbounded Couette flow). An example is presented in Fig. 2, where a surface of section for the case  $\omega = 0.5$ ,  $s = -0.5$ , and  $\lambda = 0.8$  at  $\varphi = 0$ , for which the background velocity is purely zonal and linear in  $y$  [cf. (1)]. This configuration may be of considerable geophysical importance, since several examples of strong isolated coherent vortices embedded in shear flows have been observed in planetary atmospheres.

The size of the chaotic zone grows with the amplitude of the periodic contraction–expansion cycle of the vortex; the Moore and Saffman solutions have no chaotic zones since the Hamiltonian is time independent. For a given amplitude of the  $(\varphi, \lambda)$  motion, the size of the chaotic zones generally increases with increasing  $s$  at fixed  $\omega$ , and when  $|s| > |\omega|$  the chaotic zones can open to infinity (e.g., see Fig. 1). We have found that, for  $\omega = 0$ , the “residence time” (i.e., the time before the particle escapes from the vicinity of the vortex and is carried away by the strain field) becomes extremely short—on the order of the period of the  $(\varphi, \lambda)$  motion for  $s \gtrsim 0.1$ . In general, the chaotic zones are very small when  $\omega$

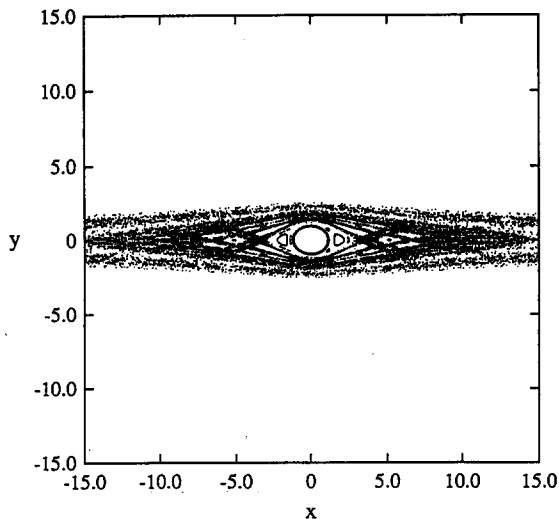


FIG. 2. The surface of section for an  $\omega = 0.5$ ,  $s = -0.5$  Kida vortex, with  $\lambda = 0.8$  at  $\varphi = 0$ . For this vortex, rotating and stretching in a simple shear, the aspect ratio varies within  $0.384\ 535\dots < \lambda < 0.8$ .

and  $s$  are larger than unity. The largest we have found for values of  $|\omega|$  and  $|s|$  is less than about  $\frac{1}{2}$  and near  $|\omega| = |s|$ .

The presence of these chaotic zones could well provide a mechanism for the recently observed<sup>10</sup> extremely complicated behavior of the vorticity filaments that are generated during the evolution of perturbed Kida vortices. We show, in Fig. 3, the evolution of a patch of dye (i.e., passive tracer) composed of  $5 \times 10^3$  particles, initially situated in a small region covering the hyperbolic stagnation point located just outside a vortex (here  $\omega = 0$ ,  $s = 0.03$ , and  $\lambda = 0.4$  at  $\varphi = 0$ ). Chaotic advection produces a large amount of mixing that spreads the dye over a broad region after only a few rotations of the vortex, even for such a small value of the background strain.

In a recent study of high-Reynolds-number two-dimensional turbulence, Benzi *et al.*,<sup>5</sup> have shown that the regions of greatest local exponential divergence of Lagrangian trajectories are found surrounding the strong coherent monopolar structures that emerge spontaneously from the initially turbulent vorticity field. These vortices are eventually well separated and the motion in their interior is very coherent,<sup>5</sup> but each one undoubtedly experiences the shear induced by the other strong vortices present in the flow. Though the observed time scale for local exponential divergence is not much smaller than the characteristic time scale for changes in the local background vorticity and strain at each vortex,<sup>5</sup> the Kida vortex with a time-independent background flow is not an unreasonable first model for the coherent structures in 2-D turbulence. Our study has shown that vortex patches in this model are often surrounded by large chaotic zones with rapid mixing, even for relatively small background shears, and that their interior is integrable. These facts are consistent with the observed stable motion inside the vortices and the presence of these large chaotic zones provides considerable insight into the observed enhanced local exponential divergence around the coherent structures.

Our study suggests that the complicated behavior of the

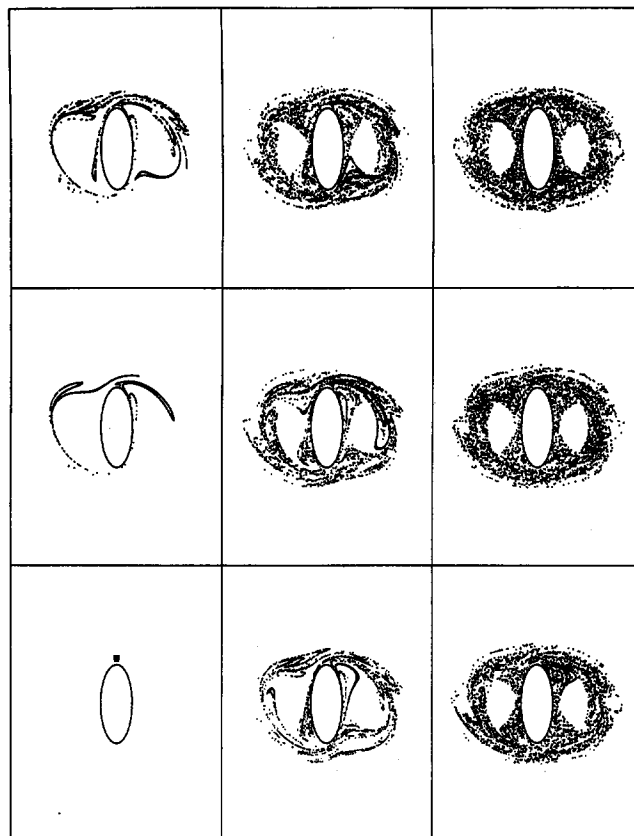


FIG. 3. The evolution of a small patch of passive tracer in the exterior field of a Kida vortex, with  $\omega = 0$ ,  $s = 0.03$ , and  $\lambda = 0.4$  at  $\varphi = 0$ . At  $t = 0$  the patch encloses the Kirchhoff unstable fixed point. The frames are plotted every two revolutions of the vortex; time advances to the right and downward. The aspect of this vortex varies in the interval  $0.343\ 041\dots < \lambda < 0.4$ .

low-level, essentially passive,<sup>4</sup> filamentary vorticity continuum that coexists with isolated coherent structures in high-Reynolds-number 2-D turbulence may result from chaotic advection and mixing induced by the coherent vortices.

#### ACKNOWLEDGMENTS

We are indebted to S. P. Meacham for illuminating us on the linear stability of the Kida solutions and wish to thank N. J. Zabusky for stimulating conversations and D. G. Dritschel for sharing his results with us before publication.

<sup>1)</sup> Department of Mathematics, Room 2-339.

<sup>2)</sup> Department of Earth, Atmospheric, and Planetary Sciences, Room 54-414.

<sup>3)</sup> B. Fornberg, *J. Comput. Phys.* **25**, 1 (1977).

<sup>4)</sup> C. Basdevant, B. Legras, R. Sadourny, and M. Beland, *J. Atmos. Sci.* **38**, 2305 (1981).

<sup>5)</sup> J. C. McWilliams, *J. Fluid Mech.* **146**, 21 (1984).

<sup>6)</sup> A. Babiano, C. Basdevant, B. Legras, and R. Sadourny, *J. Fluid Mech.* **183**, 379 (1986).

<sup>7)</sup> R. Benzi, S. Paternello, and P. Santangelo, *J. Phys. A* **21**, 1221 (1988).

<sup>8)</sup> D. G. Dritschel and B. Legras (private communication).

<sup>9)</sup> S. Kida, *J. Phys. Soc. Jpn.* **50**, 3517 (1981).

<sup>10)</sup> D. W. Moore and P. G. Saffman, in *Aircraft Wake Turbulence and its Detection* (Plenum, New York, 1971), p. 339.

<sup>9</sup>Time is scaled so that the vorticity of the patch is unity; length so that the area of the patch is  $\pi$ .

<sup>10</sup>D. G. Dritschel, *J. Fluid Mech.* (in press).

<sup>11</sup>S. P. Meacham, G. R. Flierl, and U. Send, *Dyn. Atmos. Ocean* (in press).

<sup>12</sup>H. Lamb, *Hydrodynamics* (Dover, New York, 1945), p. 159.

<sup>13</sup>V. I. Arnold, *C. R. Acad. Sci.* **261**, 17 (1965); M. Hénon, *ibid.* **262**, 312 (1966).

<sup>14</sup>H. Aref, *J. Fluid Mech.* **143**, 1 (1984).

<sup>15</sup>V. Rom-Kedar, A. Leonard, and S. Wiggins, *J. Fluid. Mech.* (in press)

<sup>16</sup>R. Bulirsch and J. Stoer, *Numerische Math.* **8**, 1 (1966).

<sup>17</sup>L. M. Polvani, G. R. Flierl, and N. J. Zabusky, *Phys. Fluids A* **1**, 18 (1989).

<sup>18</sup>M. V. Melander, J. C. McWilliams, and N. J. Zabusky, *J. Fluid Mech* **178**, 137 (1987).